Virtual Exploration of Safe Entry Zones in the Brainstem: Comprehensive Definition and Analysis of the Operative Approach

Ali Tayebi Meybodi, MD,[1,3] Benjamin K. Hendricks, MD,[1] Andrew J. Witten, BS,[2] Jerome Hartman,[1] Samuel B. Tomlinson, BA,[1] and Aaron A. Cohen-Gadol, MD, MSc, MBA[1,2]

[1]*The Neurosurgical Atlas, Indianapolis,* Indiana; [2]Department of Neurosurgery, Indiana University School of Medicine, Indianapolis, Indiana; and [3]Department of Neurosurgery, Rutgers University Medical School, Newark, New Jersey

Correspondence: Aaron A. Cohen-Gadol, MD, MSc, MBA, Indiana University, Department of Neurosurgery, 355 W 16th Street, Suite 5100, Indianapolis, IN 46202; acohenmd@gmail.com.

Short Title: 3D Models for Brainstem Safe Entry Zones

Key Words: 3D, brainstem surgery, medulla oblongata, microdissection, operative anatomy, safe entry zone, virtual model

Conflict of interest:

We have no conflicts of interest in regard to this research.

Article Type: Neurosurgical Atlas Series

This is the author's manuscript of the article published in final edited form as:

Meybodi, A. T., Hendricks, B. K., Witten, A. J., Hartman, J., Tomlinson, S. B., & Cohen-Gadol, A. A. (2020). Virtual Exploration of Safe Entry Zones in the Brainstem: Comprehensive Definition and Analysis of the Operative Approach. World Neurosurgery. https://doi.org/10.1016/j.wneu.2020.05.207

ABSTRACT

Background: Detailed and accurate understanding of intrinsic brainstem anatomy and the inter-relationship between its internal tracts and nuclei and external landmarks is of paramount importance for safe and effective brainstem surgery. Using anatomical models can be an important step in sharpening such understanding.

Objective: To show the applicability of our developed virtual 3D model in depicting the safe entry zones (SEZs) to the brainstem.

Methods: Accurate 3D virtual models of brainstem elements were created using high-resolution magnetic resonance imaging and computed tomography to depict brainstem SEZs.

Results: All the described SEZs to different aspects of the brainstem were successfully depicted using our 3D virtual models.

Conclusions: The virtual models provide an immersive experience of brainstem anatomy, allowing users to understand the intricacies of the microdissection that is necessary to appropriately traverse the brainstem nuclei and tracts toward a particular target. The models provide an unparalleled learning environment for illustrating SEZs into the brainstem that can be used for training and research.

INTRODUCTION

Historically, intrinsic brainstem lesions have been considered inoperable.[1] In the 1980s, resecting brainstem lesions gained popularity with reports of favorable outcomes.[2] A more advanced understanding of the brainstem fiber tracts enabled establishment of the so-called safe entry zones (SEZs) (Figure 1).[3-22]

An in-depth understanding of the intrinsic structural anatomy of the brainstem is critical to brainstem surgery. Such knowledge can be gathered through spending countless hours in the laboratory working on cadaveric specimens that enable fiber tract dissection.[3-22] However, developing the fine art of white matter dissection can be extremely difficult and expensive. Therefore, using accurate virtual models is an indispensable tool for sharpening this understanding. The purpose of this study was to introduce the use of virtual reality 3D models as an ancillary tool for learning the surgical anatomy of the SEZs to different regions of the brainstem.

METHODS

These methods were described previously.[13,23,24] High-resolution computed tomography and magnetic resonance imaging, as well as both 2-dimensional (2D) and 3-dimensional (3D) reconstructed catheter-based angiograms, were used to create the models. The model was used to demonstrate the topography and relationships of 19 SEZs to the brainstem (Table 1).

As an anatomic study, the present work neither required nor received institutional review board or ethics committee approval. Similarly, no patient consent was required.

Midbrain

I. Ventral and Lateral Midbrain SEZs

1. Anterior Mesencephalic Zone

<u>Topography</u>

The anterior mesencephalic zone (AMZ) (also known as the perioculomotor zone) is located on the medial one-fifth of the ventral aspect of the crus cerebri, just lateral to the root exit zone of the oculomotor nerve (Figure 2A; Model 1 [showing the mesencephalic SEZs]).[25] The AMZ harbors the frontopontine fibers and is located medial to the middle three-fifths of the crus cerebri through which the corticospinal and corticonuclear tracts pass.[13,14,26] A relatively perforator-free zone lateral to the oculomotor nerve is located between the posterior cerebral artery (PCA) superiorly, and the superior cerebellar artery (SCA) inferiorly.

Surgical Approach

The AMZ is adjacent to the medial crural cistern. The oculomotor-tentorial triangle (OTT) is the surgical window to access the AMZ.[6,14] This triangle is between the free tentorial edge and the cisternal oculomotor nerve. A pterional or orbitozygomatic craniotomy with the transsylvian pretemporal approach can be used.[24,27] The subtemporal approach with or without a tentorial incision may also be used.[27] An endoscopic endonasal transclival approach with pituitary transposition can also provide limited access to the AMZ.[24,28,29]

2. *Lateral Mesencephalic Sulcus*

Topography

The lateral mesencephalic sulcus (LMS) runs inferiorly on the lateral aspect of the midbrain between the cerebral peduncle anteriorly and the midbrain tegmentum posteriorly at the level of the inferior colliculus (surfaced by lateral lemniscus).[30,31] It extends in a rostral-caudal direction from the medial geniculate body superiorly, to join the pontomesencephalic sulcus inferiorly, and continues inferiorly between the middle and superior cerebellar peduncles as the interpeduncular sulcus. It has an average length of 9.6 ± 1.41 mm (range, 13.3–7.4 mm).[32]

A perpendicular incision in the LMS would ideally enter the midbrain anterior to the medial lemniscus (ML) and posterior to the substantia nigra (Model 1; Figure 2B).[15] The anteromedial boundary for this approach is formed by the oculomotor fibers passing through the red nucleus.[33] Extreme ventral deviation of the axial incision trajectory would hit the substantia nigra and the ventrally located pyramidal tract. Extreme dorsal deviation of the incision trajectory would damage the ML, the mesencephalic superior cerebellar peduncle fibers (and their decussation, also known as the horseshoe-shaped commissure of Wernekinck[6,14]), red nucleus, oculomotor nucleus, central tegmental tract (CTT), and the mesencephalic nucleus and tract of the trigeminal nerve.[34]

Surgical Approach

The LMS is adjacent to the posterior ambient cistern.[13,35] Approaches used to access the LMS include the subtemporal, paramedian supracerebellar infratentorial (SCIT), extreme-lateral SCIT, retrosigmoid, and presigmoid approaches.[36,37] The cerebrovascular structures encountered during this approach include the P2-PCA superiorly, the distal s2- and proximal s3-SCA, and the medial posterior choroidal artery.

II. Dorsal Midbrain SEZs

All described SEZs through the dorsal aspect of the midbrain involve the quadrigeminal plate and are adjacent to the quadrigeminal cistern.

3. Supracollicular Approach

Topography

Bricolo[14,38-42] described an SEZ just above the superior colliculi. A transverse incision is made at the subpineal triangle (triangle of Obersteiner[26]) above the superior colliculi and below the posterior commissure (Figure 2C).[43] An incision kept behind the aqueduct causes minimal damage to the mesencephalic structures. However, incising beyond the cerebral aqueduct would damage the mesencephalic nucleus and tract of the trigeminal nerve, medial longitudinal fasciculus (MLF), and oculomotor nucleus.

4. Infracollicular Approach

Topography

A transverse incision inferior to the inferior colliculi is considered safe.[24] Similar to the supracollicular zone, the infracollicular incision will access the posterior tectal region behind the cerebral aqueduct (Model 1; Figure 2C). However, one should be aware of the decussation of the trochlear nerves just below the quadrigeminal plate within the superior medullary velum.[26] An incision surpassing the cerebral aqueduct violates the trochlear nucleus, mesencephalic nucleus, and tract of the trigeminal nerve, then CTT, MLF, tectospinal tract, superior cerebral peduncle, and eventually the ML and anterolateral fasciculus.[35]

5. Intercollicular Zone

Topography

The scant intercollicular fibers between the bilateral superior and inferior colliculi enable access to lesions within the midbrain tectum dorsal to the aqueduct.[35] The main difference from the infracollicular and supracollicular approaches is the vertical trajectory of the midbrain incision in this approach (Figure 2C).[6,35]

Surgical Approach

The SCIT approach provides access to SEZs in the quadrigeminal plate.[44] Variants of the SCIT include the midline, paramedian, and extreme-lateral approaches, which have few differences regarding operative maneuverability.[6,14,45] We prefer the paramedian approach because of its less-invasive nature and the protection of the midline supracerebellar veins that it provides.

Pons

The pons is a common site for intrinsic brainstem lesions.[45-47] During resection of these lesions, the primary goal is to avoid the corticospinal, corticonuclear, and MLF tracts, as well as the nuclei and intrapontine segments of cranial nerves (CNs) V to VIII.

III. Ventral Pontine SEZs

The ventral pons is characterized by the root entry/exit zone (REZ) of CN V. Medial to CN V is the basis pontis, harboring the pyramidal tract and pontine nuclei. Lateral to trigeminal REZ, lies the middle cerebellar peduncle. Three SEZs through the region of the ventral pons have been described; they are based on 2 readily identifiable surface landmarks, CN V and CN VII to VIII REZs.[3,26,48]

6. Peritrigeminal Zone

Topography

The peritrigeminal zone (PTZ) provides access to the ventral pons via a longitudinal incision medial to a vertical line connecting the REZs of CNs V and VII to VIII with an average length of 8.9 ± 1.3 mm (range, 6.8–9.6 mm) (Figure 3A, [Model 2] showing the 3D reconstruction of pontine SEZs).[14,24] This trajectory transgresses the transverse pontine fibers and is lateral to the corticospinal tracts. It can extend as deeply as the trigeminal motor and sensory nuclei.[5,6,30] The longitudinal extent of dissection should not extend rostral to CN V or caudal to CN VII.[5,16]

The average distance between the most lateral fibers of the corticospinal tract and CN V is 4.7 ± 0.7 mm (range, 3.1–5.6 mm), which defines the medial extent of PTZ.[6] A no-fly zone of the ventral pons is described between the midline and a line connecting the lateral aspect of the cerebral peduncle and the pons.[15,31] The average distance from the lateral edge of the pyramidal tract to the CN V and VII REZs is 9.2 ± 1.2 mm (range, 7.0–11.6 mm) and 8.0 ± 1.0 mm (range, 5.6–9.6 mm), respectively.[13,15]

In contrast, entering the pons lateral to the trigeminal nerve with an axially oblique trajectory jeopardizes the intrapontine segment of CN V and its nuclei, and the ventral cochlear nucleus. [13] The trigeminal nucleus is located, on average, 10 to 12 mm (range, 9.0–16.3 mm) from the pontine surface.[13]

<u>Surgical Approach</u>

The PTZ is accessed via the retrosigmoid and presigmoid retrolabyrinthine approaches.[13,15,30] Also, anterior petrosectomy provides such access.[14,44] The endoscopic endonasal transclival approach (preferably combined with an extradural anterior petrosectomy) can also provide access to the PTZ.[13,14,44]

7. Supratrigeminal Zone

<u>Topography</u>

Hebb and Spetzler[30,31,49] introduced the transpeduncular approach to intrinsic pontine lesions. This zone is more accurately called the supratrigeminal zone (STZ), which is located above the CN V REZ lateral to the pyramidal tract (Figure 3B),[50] and is essentially the same zone described by Zenonos et al[14] as the epitrigeminal zone. To avoid the intrapontine segment of the trigeminal nerve, a tangential trajectory is suggested parallel to the direction of middle cerebellar peduncle fibers.[51] The pons is entered lateral to the CN V. Marching superior to CN V REZ, a relatively superficial intrapontine lesion can be accessed. Extending the incision too medially or too deeply would risk the pyramidal tract and the superior cerebellar peduncle, respectively. Some have described another so-called STZ approximately 4 mm below the pontomesencephalic sulcus along the sagittal-level of CN III REZ, which is technically a continuation of the AMZ in the upper pontine area.[19]

Surgical Approach

The STZ is located adjacent to the cerebellopontine cistern. Therefore, it is surgically accessed similar to PTZ. However, the STZ can also be accessed via a subtemporal transtentorial,[27,50] and the pretemporal transsylvian[14,44] approaches.

8. Lateral Pontine Zone

Topography

The medial craniocaudal extent of the approach is from the CN V REZ to that of CN VII to VIII but narrows laterally over the surface of the middle cerebellar peduncle toward the medial end of the petrosal fissure (Figure 3C). In contrast to PTZ, the LPZ is accessed by entering the pons lateral to the trigeminal-facial line. Staying relatively superficial avoids the intrapontine trigeminal fibers and nuclei.[9,15,27,35]

Surgical Approach

The LPZ is accessed through retrosigmoid and retrolabyrinthine approaches.

IV. Dorsal Pontine SEZs

Understanding dorsal pontine SEZs requires knowledge of the microanatomy of the fourth ventricular floor.[4,5,50,52]

9. Suprafacial Approach

Topography

The suprafacial (SFZ) and infrafacial (IFZ) zones were defined on the basis of the location of the facial colliculus in the rhomboid fossa.[13,20,24,35] The facial colliculus is formed by the underlying abducens nucleus and the intrapontine fibers of the facial nerve.[4,50,53,54] The suprafacial triangle located rostral to the facial colliculus comprises the SFZ (Figure 3D). The boundaries of the suprafacial triangle include the superior cerebellar peduncle laterally, the MLF medially, and the facial colliculus inferiorly.[13,35] The facial colliculus might not be visible in more than one-third of the population.[20] In such cases, the average distance from the obex to the lower pole of the facial colliculus, which is 14 to 15 mm (range, 11.5–18.0 mm), can be used.[11] Mapping of the fourth ventricular floor to localize the facial nerve can be useful.[21,55] The apex of SFZ is located at the frenulum veli,[4,56] through which the trochlear nerves pass,[11] and the average height of this triangle is 15.7 ± 2.1 mm (range, 10.8–19.2 mm).[13] The narrow base of this triangle runs between the lateral aspect of the MLF and the inferior end of the sulcus limitans at the upper border of the facial colliculus measuring 7.4 ± 0.5 mm on average (range, 5.6–10.4 mm).[11]

The rationale of limiting the lateral extension of the SFZ to sulcus limitans (and not the cerebellar peduncle) is to avoid the trigeminal mesencephalic tract and the CTT located deep to the vestibular area or the trigeminal motor and main sensory nuclei deep to the superolateral edge of the superior fovea triangle (Model 2).[11,13]

A 1-cm longitudinal incision is started caudally from the edge of the superior cerebellar peduncle and 4 to 5 mm laterally from the median sulcus[13] (to avoid the MLF, with an average width of 1 ± 0.4 mm[20]). The deep limit of the SFZ is the ML, which is 4.5 mm from the ependymal surface.[13] Any lesion located deeper than 4 mm to the floor of the fourth ventricle would likely be anterior to the ML and would not be amenable to an SFZ approach. Any viable neuronal tissue overlying the lesion on magnetic resonance imaging on the floor of the fourth ventricle necessitates a peritrigeminal pathway, because even minor neuronal tissue on the floor can be highly functional.

10. Infrafacial Approach

<u>Topography</u>

The IFZ uses the interval between the intrapontine segment of the facial nerve superiorly, which is at the level of a transverse line passing through the upper edges of the lateral recesses of the fourth ventricle[20,50,54,56], the MLF medially, and the hypoglossal and dorsal vagal nuclei inferiorly,[13] with an average rostrocaudal dimension of 6 to 9 mm (Figure 3D).[53,55] At the lower margin of the lateral recess, the facial and ambiguous nuclei are located just lateral to the medial-most point of the tela choroidea, and IFZ should be entered medial to this point.[13,53] The lower limit of IFZ corresponds to the lower edge of the lateral recess or the upper strands of the striae medullares.[13] When the striae medullares are not visible, the distance between the obex and the upper pole of the hypoglossal triangle can be used (range, 6.5–10.6 mm).[11,13,20] The ventral limit of IFZ is the CTT, which is reached at an average depth of 4.9 mm from the ependymal surface.[11,13,53] Kyoshima et al[13] described an ependymal incision just above the striae medullares, approximately 4 to 5 mm lateral to the median sulcus. The incision should be as small as possible (≤6 mm) to avoid injuring the facial colliculus.

11. Median Sulcus of the Fourth Ventricle

<u>Topography</u>

Described by Bricolo,[20] the median sulcus (MS-IV) runs between the bilateral median eminences (also known as funiculi teres[26]) with underlying MLFs that do not have crossing fibers above the level of the facial colliculi.[43] Therefore, the MS is used above the facial colliculi (Figure 3D). The downside of this approach is that any lateral retraction would cause damage to the MLF.

<u>Surgical Approach</u>

Access to the SFZ, IFZ, and MS-IV requires a midline suboccipital transvermian or telovelar approach.[13]

12. Area Acustica

<u>Topography</u>

Bricolo[4] described the area acustica (AA) over the dorsal aspect of the lateral recess of the fourth ventricle. This zone corresponds to the inferior cerebellar peduncle fibers located underneath the lateral end of the dorsal acoustic striae (i.e., striae medullares) (Figure 3D). At this level, the peduncular fibers are ventral to the dorsal cochlear nucleus and dorsal to the spinal tract of the trigeminal nerve. This area is a few millimeters superior to the lateral medullary zone (LMZ) (corresponding to a more inferiorly located part of the inferior cerebellar peduncle[26]; see "Lateral Medullary Zone"). The surgical corridor through the AA should be kept shallow, because deep to the inferior cerebellar peduncle, the following (from dorsal to ventral) will be reached: trigeminal spinal tract, nucleus ambiguus, and facial nucleus.[7] Evidently, the dorsal cochlear nucleus and the peduncular fibers would be breached after entering the AA.

13. Floccular Peduncle

Topography

The floccular peduncle (FP) is a potential SEZ along the rostral wall of the lateral recess of the fourth ventricle, rostral to the floccular attachment of the inferior medullary velum (Figure 3D).[57,58] The FP simply forms the roof of the lateral recess along the attachment of the inferior medullary velum. The approximate length of the FP is 8.0 mm (range, 5.2–9.3 mm).[8] No clinical correlate was provided by the authors.

Surgical Approach

The AA and FP can be reached through exposure of the lateral end of the lateral recess from the ventricular side, which can be done by using a suboccipital telovelar approach. As an alternative, a trans-tonsillobiventral fissure or trans-tonsillouvular fissure approach can be used to reach the lateral recess of the fourth ventricle.[13]

Medulla Oblongata

V. Ventral and Lateral Medullary SEZs

14. Anterolateral Sulcus

Topography

The bilateral anterolateral sulci (ALS) form the lateral boundary of the medullary pyramids and reach the pontomedullary sulcus just anterior to the supraolivary fossette (Model 3; Figure 4A). It is continuous inferiorly with the ALS of the spinal cord. The ALS forms REZs for CN XII and motor roots of the spinal cord. At the level of the olive, the ALS is called the preolivary sulcus. The ALS approach requires an oblique trajectory through the preolivary sulcus between the caudal-most roots of CN XII and the rostral-most rootlets of the C1 nerve.[8] The tracts at risk are the anterolateral fascicle, olivary amiculum and internal arcuate fibers laterally, and the ML and MLF medially.[6,16]

15. Olivary Zone

Topography

The olivary zone (OZ) is approached similar to the ALS. The trajectory involves a neurotomy in the medullary olive (Figure 4A).[30,31] The olive has a craniocaudal length of 13.5 mm and a width of 7.0 mm.[4,50] The average distance from the pial surface on the olive to the point at which deep fiber groups enter its hilus is 5.5 ± 0.5 mm (range, 4.7–6.9 mm).[15] Deeply, the intramedullary segment of CN XII is encountered.[15]

16. Posterolateral Sulcus

Topography

The posterolateral sulcus (PLS) corresponds to the postolivary sulcus and marks the posterior limit of the olive on the anterolateral aspect of the medulla. The rootlets of CNs IX to X originate dorsolateral to this sulcus (Figure 4A). The spinal tract of the trigeminal nerve intersects with the intramedullary segment of CNs IX to X.[35]

Surgical Approach

The ALS is appropriate for exophytic lesions that involve the caudal anterolateral medulla, adjacent to the lateral medullary cistern.[35] This region can be accessed using the far-lateral approach. The medullary olive and lower CNs serve as the landmarks.[6] An endoscopic endonasal approach to remove the lower third of the clivus and anterior part of the occipital condyle exposes the ALS.[24] The surgical exposure of OZ and PLS is similar to that of ALS, although endoscopic approaches provide limited exposure of the PLS.

17. Lateral Medullary Zone

Topography

Deshmukh et al[4,5] described the approach through the lateral medullary zone (LMZ), to access the rostral dorsolateral medulla. The LMZ corresponds to the rostrolateral part of the inferior cerebellar peduncle ventral to the foramen of Luschka and REZs of CNs IX to X (Figure 4B). At the level of the rostral medulla, the floor of the fourth ventricle is lined by several nuclei and tracts. The nuclei include (medially to laterally) the hypoglossal, the dorsal vagal, the medial and vestibular, the lateral cuneate, and, more rostrally, dorsal cochlear nuclei.[7] Important tracts include (medially to laterally) the dorsal longitudinal fasciculus, the solitary fasciculus, and the lateral vestibulospinal tract.[7,35]

Surgical Approach

The LMZ can be accessed through a retrosigmoid craniotomy, although the far-lateral and presigmoid approaches can also be used. A vertical neurotomy is made on the inferior cerebellar peduncle, posterior to the origin of CNs IX to X.[7]

VI. Dorsal Medullary SEZs

18. Posterior Median Sulcus

Topography

The posterior median sulcus (PMS) is entered along the midline below the level of the obex (Figure 4B).[14] The corridor is developed between the gracile fascicles/tubercles (clava) on the dorsal aspect of the medulla. The hypoglossal and dorsal vagal nuclei are located near the midline (average, 0.3 mm; range, 0.2–0.4 mm),[4,5,16,26,50] and lateral retraction of the neural tissue should be avoided when using PMS.

19. Posterior Intermediate Sulcus

Topography

The posterior intermediate sulcus (PIS) runs between the gracile and cuneate tubercles/fascicles (Figure 4B).[53] Deepening the surgical corridor along the PIS puts the hypoglossal and dorsal vagal nuclei at risk.[5,26] These nuclei are reached even dorsal to the central canal and its most rostral dilatation just inferior to the obex (Arancio's ventricle).[53] The trigeminal spinal tract is located ventrolateral to the cuneate fascicle and descends down the upper spinal cord and might be at risk.[43]

Surgical Approach

The PMS and PIS can be approached via a median suboccipital craniotomy and C1 laminectomy.

USE OF VIRTUAL REALITY MODELS IN UNDERSTANDING THE OPERATIVE ANATOMY OF THE BRAINSTEM

We have shown the applicability of our 3D brainstem models in demonstrating the complex surgical anatomy of brainstem SEZs. Models are an integral part of teaching anatomy. They have been created and used since the 18th century, after publication of Morgagni's masterpiece *De Sedibus et Causis Morborum* in 1761.[13,35] Today, many medical educators use physical and/or digital 3D models to depict anatomical interrelationships that can be even more efficient and flexible than cadaver specimens while avoiding financial, institutional, ethical, and social limitations of cadaver use. [59-62]

Importance of Digital 3D Models in Depicting Surgical Anatomy of the Brainstem

When removing a symptomatic lesion that does not reach the pial surface, the surgeon should choose a port of entry with the minimal untoward complications. Achieving this goal requires knowledge of the internal structure of the brainstem as a see-through image that does not lose accuracy with perspective changes (i.e., different approaches). Extracted brains are usually used to study the external features of the brainstem. Further ahead, sectional anatomy of the brainstem should be analyzed. However, special tissue preparation is needed to reliably identify various tracts and nuclei. Even so, it is difficult to obtain a flawless mental see-through through sectional studies.

Therefore, the application of accurate detailed digital 3D models that provide an interactive interface can be helpful in understanding this complexity. Our digital 3D models of the brainstem provide these features. The interactivity of our proposed models enables trainees to study the surgical anatomy of the brainstem and to understand the interrelationship between various internal structures, as well as the relationship between those structures and surface landmarks and vascular anatomy. Furthermore, the ability to turn and rotate the models enables trainees to visualize these relationships with the surgical positioning implemented. These features are extremely important in preparing neurosurgical trainees for complex surgical approaches to the brainstem for which patient positioning can disrupt the orthogonal understanding of anatomy. Indeed, the extent to which this model can enhance trainees' understanding of brainstem anatomy is subject to further analysis. Another important potential advantage of digital 3D models of the brainstem (not yet present in our model) is the ability to add intrinsic lesions that could recapitulate tract distortions with lesional enlargement.

CONCLUSION

With detailed neuroanatomic evaluation, advancement in stereotactic neuronavigation and operative microscopic technology, safe neurosurgical procedures in the brainstem have become possible through SEZs. Using advanced computer modeling, we were able to illustrate these SEZs within a virtual 3D environment. This experience offers a superb learning environment for clinical, research, and educational purposes.

ACKNOWLEDGMENTS

We appreciate the generous support of the Samerian Foundation for the completion of this work.

This research did not receive any specific grant from funding agencies in the public, commercial, or not-for-profit sectors.

REFERENCES

1. Ingraham FD, Matson DD. *Neurosurgery of infancy and childhood.* Springfield, Ill.,: Thomas; 1954.
2. Lassiter KR, Alexander E, Jr., Davis CH, Jr., Kelly DL, Jr. Surgical treatment of brain stem gliomas. *J Neurosurg.* 1971;34(6):719-725.
3. Porter RW, Detwiler PW, Spetzler RF, et al. Cavernous malformations of the brainstem: experience with 100 patients. *J Neurosurg.* 1999;90(1):50-58.
4. Bertalanffy H, Benes L, Miyazawa T, Alberti O, Siegel AM, Sure U. Cerebral cavernomas in the adult. Review of the literature and analysis of 72 surgically treated patients. *Neurosurg Rev.* 2002;25(1-2):1-53; discussion 54-55.
5. Giliberto G, Lanzino DJ, Diehn FE, Factor D, Flemming KD, Lanzino G. Brainstem cavernous malformations: anatomical, clinical, and surgical considerations. *Neurosurg Focus.* 2010;29(3):E9.
6. Yagmurlu K, Rhoton AL, Tanriover N, Bennett JA. Three-Dimensional Microsurgical Anatomy and the Safe Entry Zones of the Brainstem. *Operative Neurosurgery.* 2014;10(4):602-620.
7. Deshmukh VR, Rangel-Castilla L, Spetzler RF. Lateral inferior cerebellar peduncle approach to dorsolateral medullary cavernous malformation. *J Neurosurg.* 2014;121(3):723-729.
8. Akiyama O, Matsushima K, Nunez M, et al. Microsurgical anatomy and approaches around the lateral recess with special reference to entry into the pons. *J Neurosurg.* 2018;129(3):740-751.
9. Baghai P, Vries JK, Bechtel PC. Retromastoid approach for biopsy of brain stem tumors. *Neurosurgery.* 1982;10(5):574-579.

10. Bhardwaj RD, Auguste KI, Kulkarni AV, Dirks PB, Drake JM, Rutka JT. Management of pediatric brainstem cavernous malformations: experience over 20 years at the hospital for sick children. *J Neurosurg Pediatr.* 2009;4(5):458-464.
11. Bogucki J, Gielecki J, Czernicki Z. The anatomical aspects of a surgical approach through the floor of the fourth ventricle. *Acta Neurochir (Wien).* 1997;139(11):1014-1019.
12. Strauss C. The anatomical aspects of a surgical approach through the floor of the fourth ventricle. *Acta Neurochir (Wien).* 1998;140(10):1099.
13. Yagmurlu K, Rhoton AL, Jr., Tanriover N, Bennett JA. Three-dimensional microsurgical anatomy and the safe entry zones of the brainstem. *Neurosurgery.* 2014;10 Suppl 4:602-619; discussion 619-620.
14. Cavalcanti DD, Preul MC, Kalani MY, Spetzler RF. Microsurgical anatomy of safe entry zones to the brainstem. *J Neurosurg.* 2016;124(5):1359-1376.
15. Recalde RJ, Figueiredo EG, de Oliveira E. Microsurgical anatomy of the safe entry zones on the anterolateral brainstem related to surgical approaches to cavernous malformations. *Neurosurgery.* 2008;62(3 Suppl 1):9-15; discussion 15-17.
16. Cantore G, Missori P, Santoro A. Cavernous angiomas of the brain stem. Intra-axial anatomical pitfalls and surgical strategies. *Surg Neurol.* 1999;52(1):84-93; discussion 93-84.
17. Fahlbusch R, Strauss C, Huk W, Rockelein G, Kompf D, Ruprecht KW. Surgical removal of pontomesencephalic cavernous hemangiomas. *Neurosurgery.* 1990;26(3):449-456; discussion 456-447.

18. Ferroli P, Sinisi M, Franzini A, Giombini S, Solero CL, Broggi G. Brainstem cavernomas: long-term results of microsurgical resection in 52 patients. *Neurosurgery.* 2005;56(6):1203-1212; discussion 1212-1204.

19. Hebb MO, Spetzler RF. Lateral transpeduncular approach to intrinsic lesions of the rostral pons. *Neurosurgery.* 2010;66(3 Suppl Operative):26-29; discussion 29.

20. Kyoshima K, Kobayashi S, Gibo H, Kuroyanagi T. A study of safe entry zones via the floor of the fourth ventricle for brain-stem lesions. Report of three cases. *J Neurosurg.* 1993;78(6):987-993.

21. Lang J, Jr., Ohmachi N, Lang J, Sr. Anatomical landmarks of the Rhomboid fossa (floor of the 4th ventricle), its length and its width. *Acta Neurochir (Wien).* 1991;113(1-2):84-90.

22. Yang Y, van Niftrik B, Ma X, et al. Analysis of safe entry zones into the brainstem. *Neurosurg Rev.* 2019.

23. Ludwig E, Klingler J. *Atlas cerebri humani. Der innere Bau des Gehirns dargestellt auf Grund makroskopischer Präparate. The inner structure of the brain demonstrated on the basis of macroscopical preparations.* Boston,: Little, Brown; 1956.

24. Parraga RG, Possatti LL, Alves RV, Ribas GC, Ture U, de Oliveira E. Microsurgical anatomy and internal architecture of the brainstem in 3D images: surgical considerations. *J Neurosurg.* 2016;124(5):1377-1395.

25. Hendricks BK, Patel AJ, Hartman J, Seifert MF, Cohen-Gadol A. Operative Anatomy of the Human Skull: A Virtual Reality Expedition. *Oper Neurosurg (Hagerstown).* 2018;15(4):368-377.

26. Bricolo A. Surgical management of intrinsic brain stem gliomas. *Oper Tech Neurosurg.* 2000;3(2):137-154.

27. Tayebi Meybodi A, Gandhi S, Mascitelli J, et al. The oculomotor-tentorial triangle. Part 1: microsurgical anatomy and techniques to enhance exposure. *J Neurosurg.* 2018:1-9.

28. McLaughlin N, Ma Q, Emerson J, Malkasian DR, Martin NA. The extended subtemporal transtentorial approach: the impact of trochlear nerve dissection and tentorial incision. *J Clin Neurosci.* 2013;20(8):1139-1143.

29. Cavalcanti DD, Morais BA, Figueiredo EG, Spetzler RF, Preul MC. Accessing the Anterior Mesencephalic Zone: Orbitozygomatic Versus Subtemporal Approach. *World Neurosurg.* 2018;119:e818-e824.

30. Weiss A, Perrini P, De Notaris M, et al. Endoscopic Endonasal Transclival Approach to the Ventral Brainstem: Anatomic Study of the Safe Entry Zones Combining Fiber Dissection Technique with 7 Tesla Magnetic Resonance Guided Neuronavigation. *Oper Neurosurg (Hagerstown).* 2019;16(2):239-249.

31. Essayed WI, Singh H, Lapadula G, Almodovar-Mercado GJ, Anand VK, Schwartz TH. Endoscopic endonasal approach to the ventral brainstem: anatomical feasibility and surgical limitations. *J Neurosurg.* 2017;127(5):1139-1146.

32. Ardeshiri A, Ardeshiri A, Linn J, Tonn JC, Winkler PA. Microsurgical anatomy of the mesencephalic veins. *J Neurosurg.* 2007;106(5):894-899.

33. Duvernoy HM. *Human brainstem vessels.* Berlin ; New York: Springer-Verlag; 1978.

34. Voogd J, van Baarsen K. The horseshoe-shaped commissure of Wernekinck or the decussation of the brachium conjunctivum methodological changes in the 1840s. *Cerebellum.* 2014;13(1):113-120.

35. Nieuwenhuys R, Voogd J, Huijzen Cv. *The human central nervous system.* 4th ed. New York: Springer; 2008.

36. Rhoton AL. The posterior fossa cisterns. *Neurosurgery.* 2000;47(3 Suppl):S287-297.

37. Inoue K, Seker A, Osawa S, Alencastro LF, Matsushima T, Rhoton AL, Jr. Microsurgical and endoscopic anatomy of the supratentorial arachnoidal membranes and cisterns. *Neurosurgery.* 2009;65(4):644-664; discussion 665.

38. Cavalcanti DD, Morais BA, Figueiredo EG, Spetzler RF, Preul MC. Surgical approaches for the lateral mesencephalic sulcus. *J Neurosurg.* 2019:1-6.

39. Kalani MYS, Couldwell WT. Extreme Lateral Supracerebellar Infratentorial Approach to the Lateral Midbrain. *J Neurol Surg B Skull Base.* 2018;79(Suppl 5):S415-S417.

40. de Oliveira JG, Lekovic GP, Safavi-Abbasi S, et al. Supracerebellar infratentorial approach to cavernous malformations of the brainstem: surgical variants and clinical experience with 45 patients. *Neurosurgery.* 2010;66(2):389-399.

41. Jittapiromsak P, Little AS, Deshmukh P, Nakaji P, Spetzler RF, Preul MC. Comparative analysis of the retrosigmoid and lateral supracerebellar infratentorial approaches along the lateral surface of the pontomesencephalic junction: a different perspective. *Neurosurgery.* 2008;62(5 Suppl 2):ONS279-287: discussion ONS287-278.

42. Vishteh AG, David CA, Marciano FF, Coscarella E, Spetzler RF. Extreme lateral supracerebellar infratentorial approach to the posterolateral mesencephalon: technique and clinical experience. *Neurosurgery.* 2000;46(2):384-388; discussion 388-389.

43. Testut L, Latarjet A. *Tratado de Anatomia Humana: Tomo II.* Vol 2. Barcelona: Salvat Editores; 1984.

44. Kalani MY, Yagmurlu K, Martirosyan NL, Cavalcanti DD, Spetzler RF. Approach selection for intrinsic brainstem pathologies. *J Neurosurg.* 2016;125(6):1596-1607.

45. Cavalcanti DD, Morais BA, Figueiredo EG, Spetzler RF, Preul MC. Supracerebellar Infratentorial Variant Approaches to the Intercollicular Safe Entry Zone. *World Neurosurg.* 2019;122:e1285-e1290.

46. Ammirati M, Bernardo A, Musumeci A, Bricolo A. Comparison of different infratentorial-supracerebellar approaches to the posterior and middle incisural space: a cadaveric study. *J Neurosurg.* 2002;97(4):922-928.

47. Kulwin C, Matsushima K, Malekpour M, Cohen-Gadol AA. Lateral supracerebellar infratentorial approach for microsurgical resection of large midline pineal region tumors: techniques to expand the operative corridor. *J Neurosurg.* 2016;124(1):269-276.

48. Garcia RM, Ivan ME, Lawton MT. Brainstem cavernous malformations: surgical results in 104 patients and a proposed grading system to predict neurological outcomes. *Neurosurgery.* 2015;76(3):265-277; discussion 277-268.

49. d'Avella E, Angileri F, de Notaris M, et al. Extended endoscopic endonasal transclival approach to the ventrolateral brainstem and related cisternal spaces: anatomical study. *Neurosurg Rev.* 2014;37(2):253-260; discussion 260.

50. Cavalheiro S, Yagmurlu K, da Costa MD, et al. Surgical approaches for brainstem tumors in pediatric patients. *Childs Nerv Syst.* 2015;31(10):1815-1840.

51. Zenonos GA, Fernandes-Cabral D, Nunez M, Lieber S, Fernandez-Miranda JC, Friedlander RM. The epitrigeminal approach to the brainstem. *J Neurosurg.* 2018;128(5):1512-1521.

52. Hauck EF, Barnett SL, White JA, Samson D. The presigmoid approach to anterolateral pontine cavernomas. Clinical article. *J Neurosurg.* 2010;113(4):701-708.

53. Strauss C, Lutjen-Drecoll E, Fahlbusch R. Pericollicular surgical approaches to the rhomboid fossa. Part I. Anatomical basis. *J Neurosurg.* 1997;87(6):893-899.

54. Strauss C, Romstock J, Fahlbusch R. Pericollicular approaches to the rhomboid fossa. Part II. Neurophysiological basis. *J Neurosurg.* 1999;91(5):768-775.

55. Strauss C, Fahlbusch R. Anatomical aspects for surgery within the floor of the IVth ventricle. *Zentralbl Neurochir.* 1997;58(1):7-12.

56. Bertalanffy H, Tissira N, Krayenbuhl N, Bozinov O, Sarnthein J. Inter- and intrapatient variability of facial nerve response areas in the floor of the fourth ventricle. *Neurosurgery.* 2011;68(1 Suppl Operative):23-31; discussion 31.

57. Tayebi Meybodi A, Lawton MT, Tabani H, Benet A. Tonsillobiventral fissure approach to the lateral recess of the fourth ventricle. *J Neurosurg.* 2017;127(4):768-774.

58. Aydin I, Hanalioglu S, Peker HO, et al. The Tonsillouvular Fissure Approach: Access to Dorsal and Lateral Aspects of the Fourth Ventricle. *World Neurosurg.* 2018;114:e1107-e1119.

59. Pawlina W, Drake RL. Anatomical models: don't banish them from the anatomy laboratory yet. *Anat Sci Educ.* 2013;6(4):209-210.

60. Riva A, Conti G, Solinas P, Loy F. The evolution of anatomical illustration and wax modelling in Italy from the 16th to early 19th centuries. *J Anat.* 2010;216(2):209-222.

61. Ballestriero R. Anatomical models and wax Venuses: art masterpieces or scientific craft works? *J Anat.* 2010;216(2):223-234.

62. Fredieu JR, Kerbo J, Herron M, Klatte R, Cooke M. Anatomical Models: a Digital Revolution. *Med Sci Educ.* 2015;25(2):183-194.

Figure 1. Artist's illustration of the most commonly used safe entry zones to intrinsic brainstem lesions. With permission from *The Neurosurgical Atlas* by Aaron Cohen-Gadol, MD.

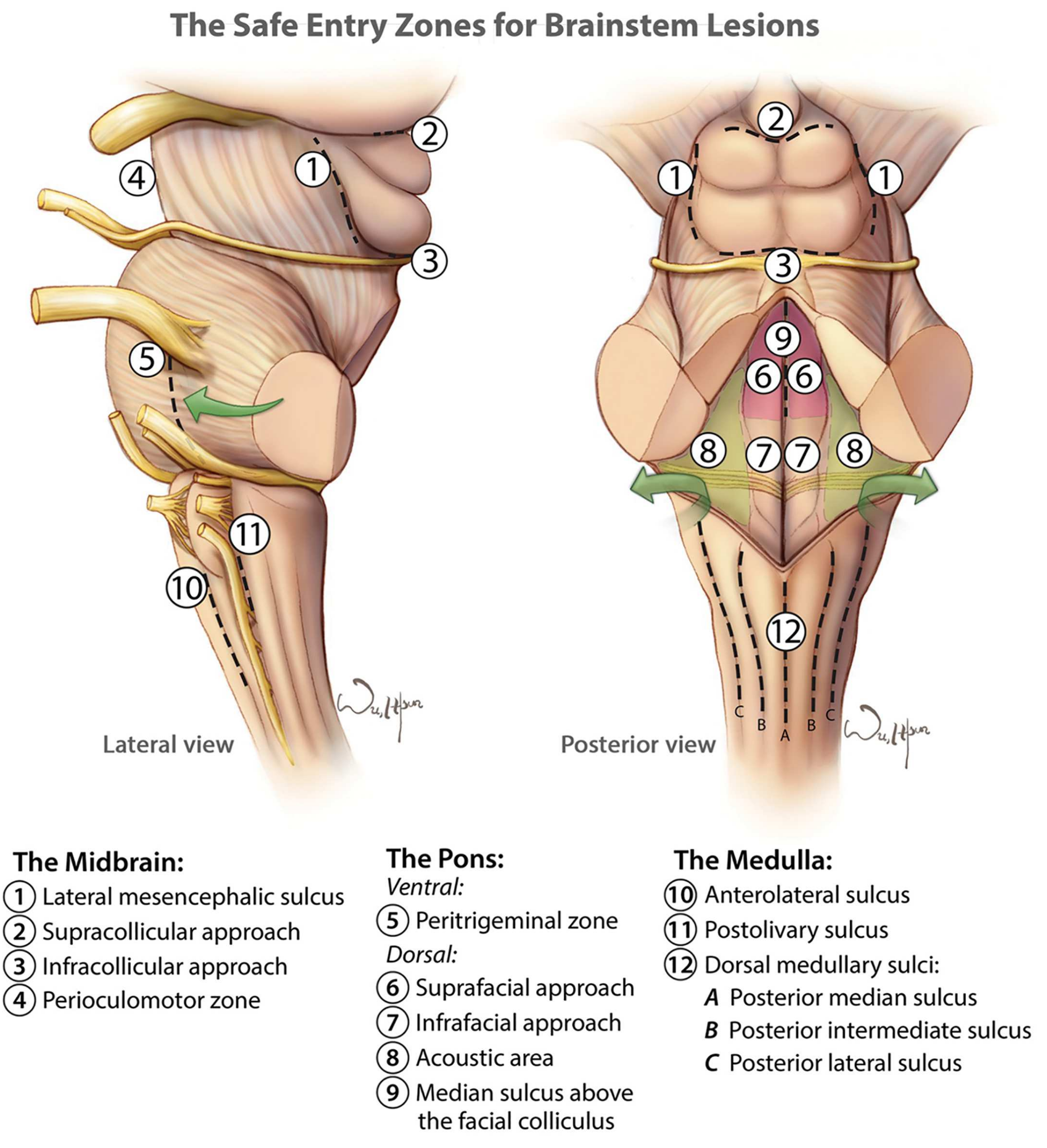

Figure 2. Three-dimensional model snapshots of safe entry zones (SEZs) to the midbrain; the SEZs are shown as green-shaded areas. **A,** Approach trajectory to the anterior mesencephalic zone (between the PCA and SCA) is indicated by the green arrow. **B,** Lateral medullary sulcus (LMS). Note that the LMS is continuous inferiorly with the interpeduncular sulcus (IPS) between the middle cerebellar peduncle (MCP) and the superior cerebellar peduncle (SCP). **C,** Dashed lines show the SEZ in the pericollicular area in the tectal region. 1, supracollicular zone; 2, infracollicular zone; 3, intercollicular zone; CN, cranial nerve; IC, inferior colliculus; PCA, posterior cerebral artery; PCoA, posterior communicating artery; PMS, pontomesencephalic sulcus; SC, superior colliculus; SCA, superior cerebellar artery. With permission from *The Neurosurgical Atlas* by Aaron Cohen-Gadol, MD.

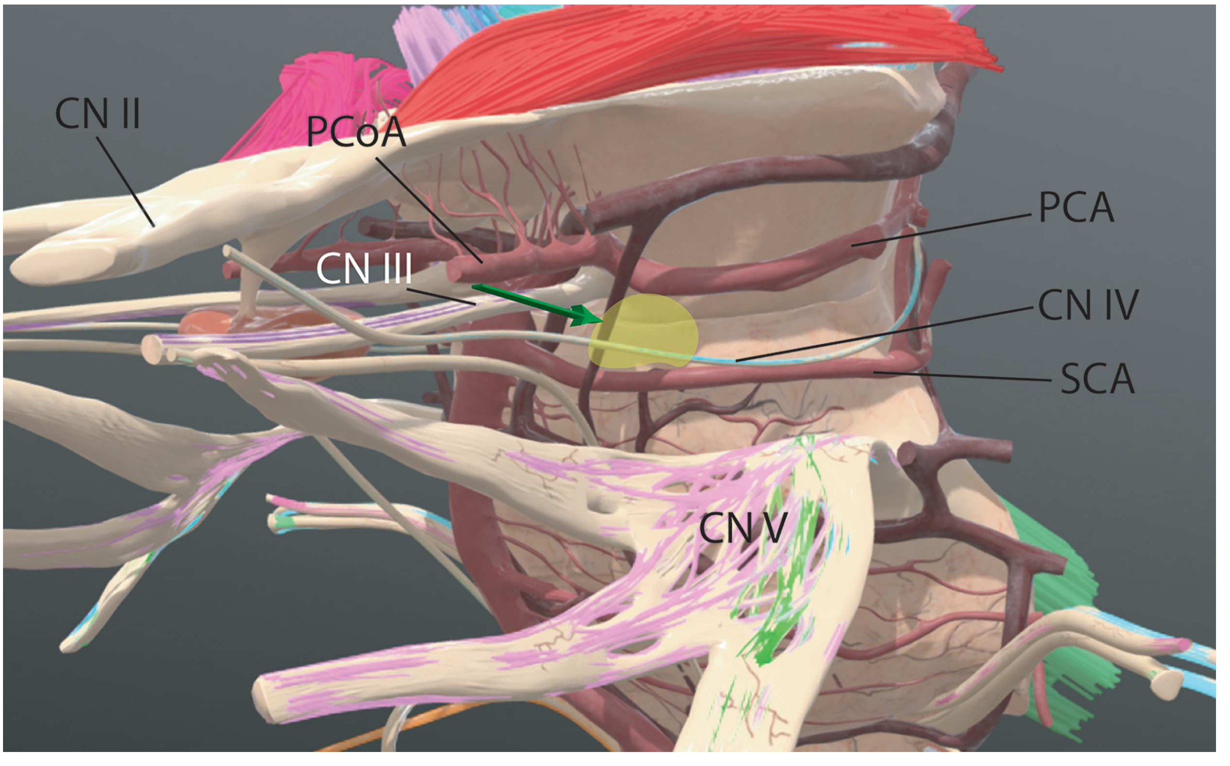

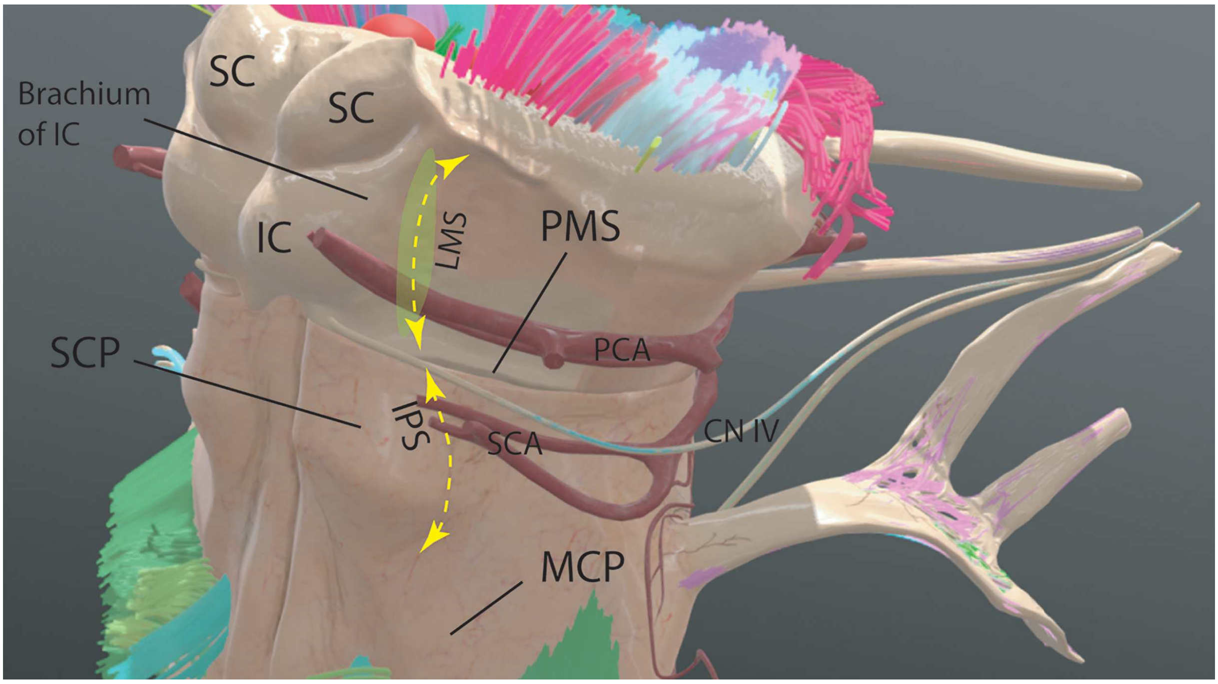
SC
SC
Brachium
of IC
IC
LMS
PMS
SCP
PCA
IPS
SCA
CN IV
MCP

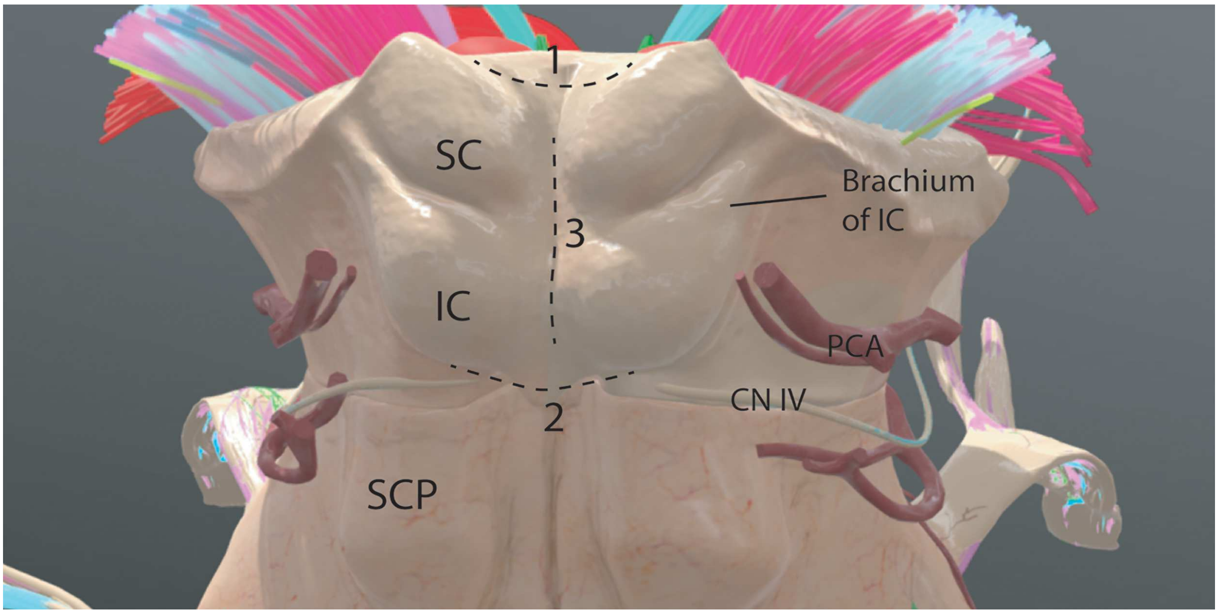
1
SC
Brachium
of IC
3
IC
PCA
CN IV
2
SCP

Figure 3. Three-dimensional model snapshots of safe entry zones (SEZs) to the pons. **A,** Peritrigeminal zone (PTZ), located just anteromedial to a line connecting the root entry/exit zone (REZs) of cranial nerves (CNs) V and VII through VIII. **B,** Supratrigeminal zone (STZ), located just superolateral to the REZ of CN V, with the approach trajectory almost tangential to the surface parallel to superior cerebellar peduncle (SCP) fibers (red arrow). **C,** Lateral trigeminal zone (LPZ), located just lateral to the line connecting the REZs of CNs V and VII through VIII. The approach trajectory is shown with a red arrow. **D,** Dorsal pontine SEZ with the fourth ventricle unroofed to facilitate visualization of the floor. The blue arrow shows the directionality of the lateral recess of the fourth ventricle. AA, area acoustica; AICA, anterior inferior cerebellar artery; BA, basilar artery; FC, facial colliculus; FP, floccular peduncle; HT, hypoglossal triangle; ICP, inferior cerebellar peduncle; IFZ, infrafacial zone; MCP, middle cerebellar peduncle; PCA, posterior cerebral artery; SCA, superior cerebellar artery; SFT, superior fovea triangle; SFZ, suprafacial zone; VT, vagal triangle. With permission from *The Neurosurgical Atlas* by Aaron Cohen-Gadol, MD.

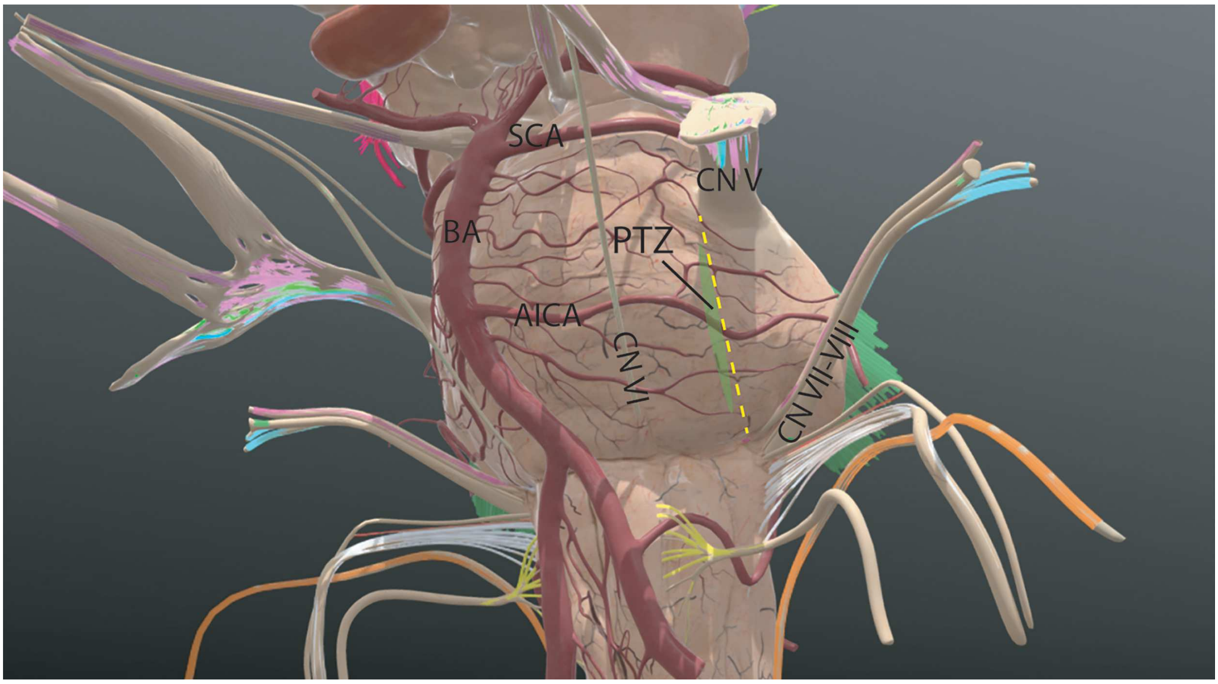

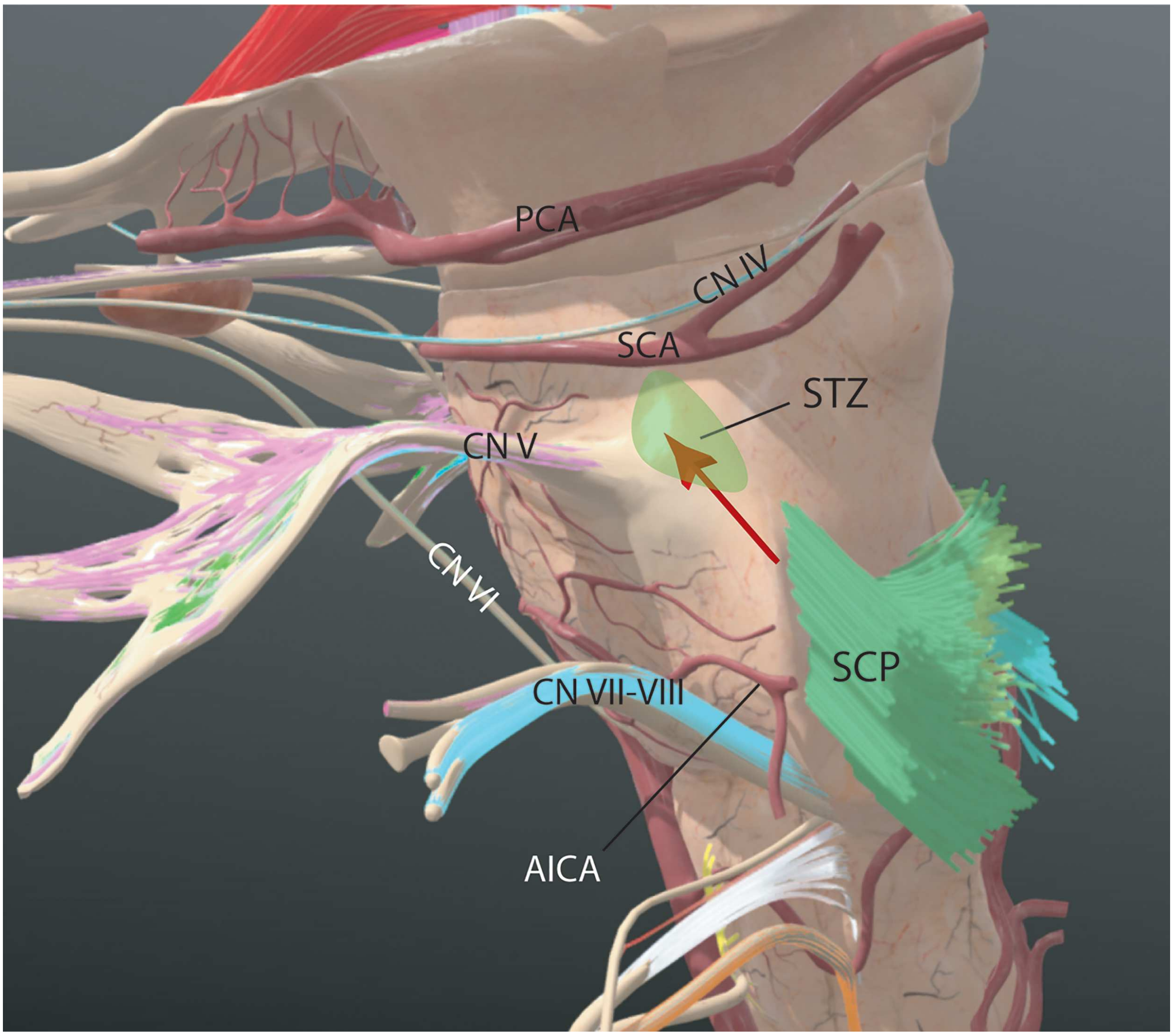
PCA
CN IV
SCA
STZ
CN V
CN VI
SCP
CN VII-VIII
AICA

623 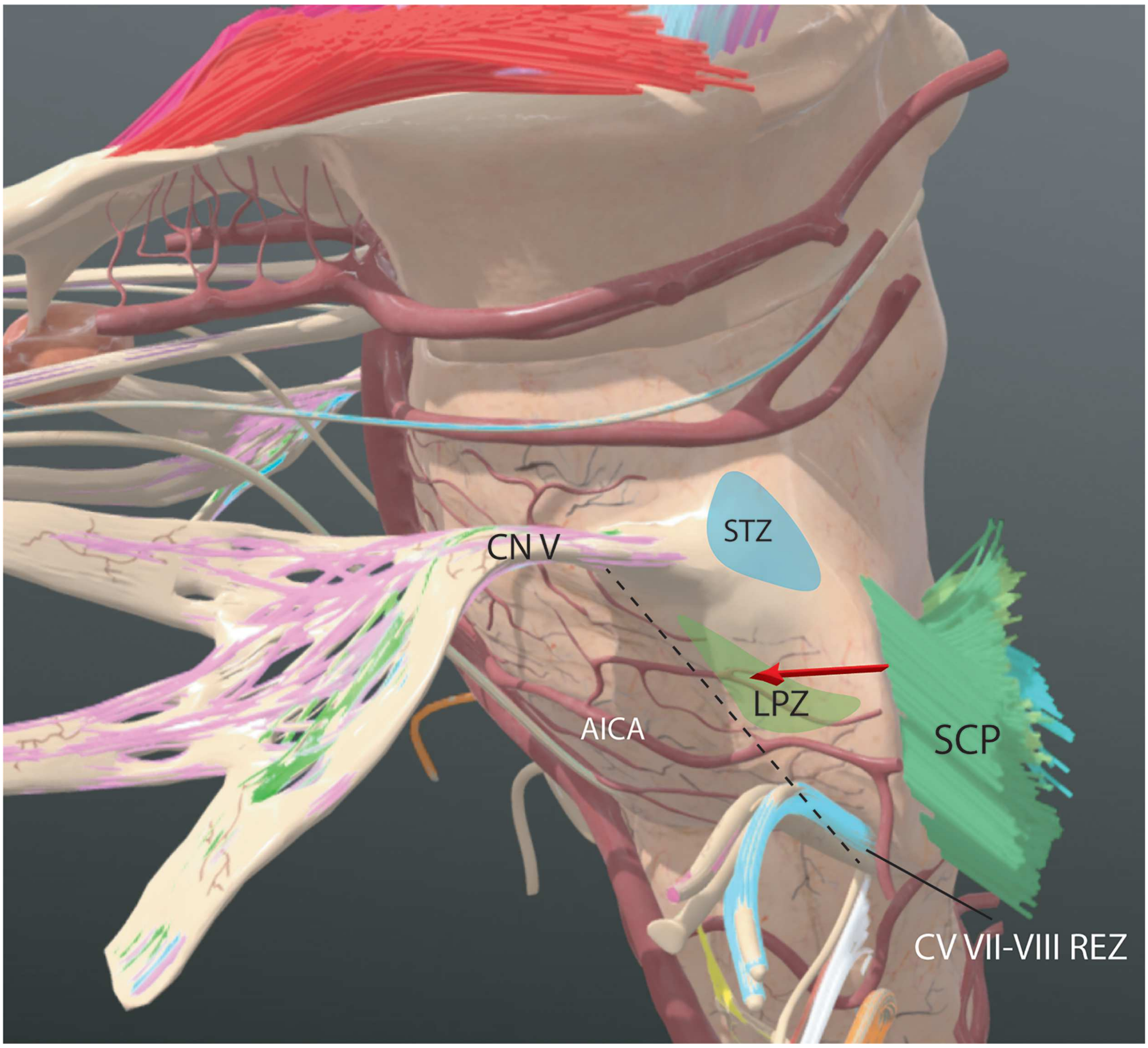

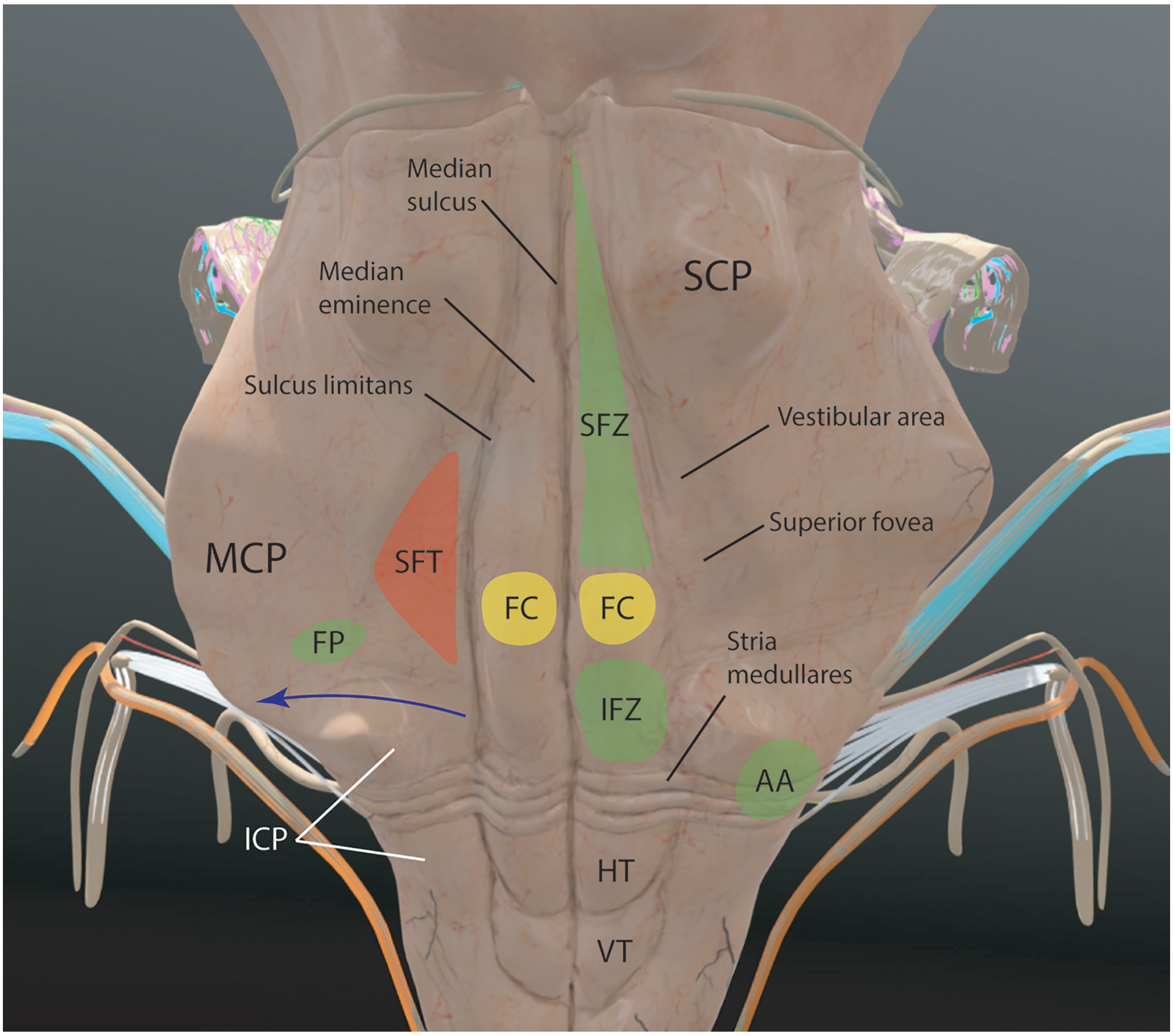

Median
sulcus
Median
eminence
Sulcus limitans
SCP
SFZ
Vestibular area
Superior fovea
MCP
SFT
FC
FC
FP
Stria
medullares
IFZ
AA
ICP
HT
VT

Figure 4. Three-dimensional model snapshots of safe entry zones (SEZs) to the medulla. **A,** Right ventrolateral perspective of the lower brainstem showing the following ventral and lateral SEZs of the medulla: olivary zone (OZ), anterolateral sulcus (ALS), and posterolateral sulcus (PLS). Note that the preolivary sulcus (POS) is continuous with the ALS inferiorly. The PLS is a few millimeters anterior to the root entry/exit zone of cranial nerves (CNs) IX and X. **B,** Right dorsolateral perspective of the medulla showing the lateral medullary zone (LMZ), posterior median sulcus (PMS), and posterior intermediate zone (PIS). CT, cuneate tubercle; GT, gracile tubercle; HT, hypoglossal triangle; ICP, inferior cerebellar peduncle; OZ, olivary zone; Py, pyramid; SOF, supraolivary fossette; VT, vagal triangle. With permission from *The Neurosurgical Atlas* by Aaron Cohen-Gadol, MD.

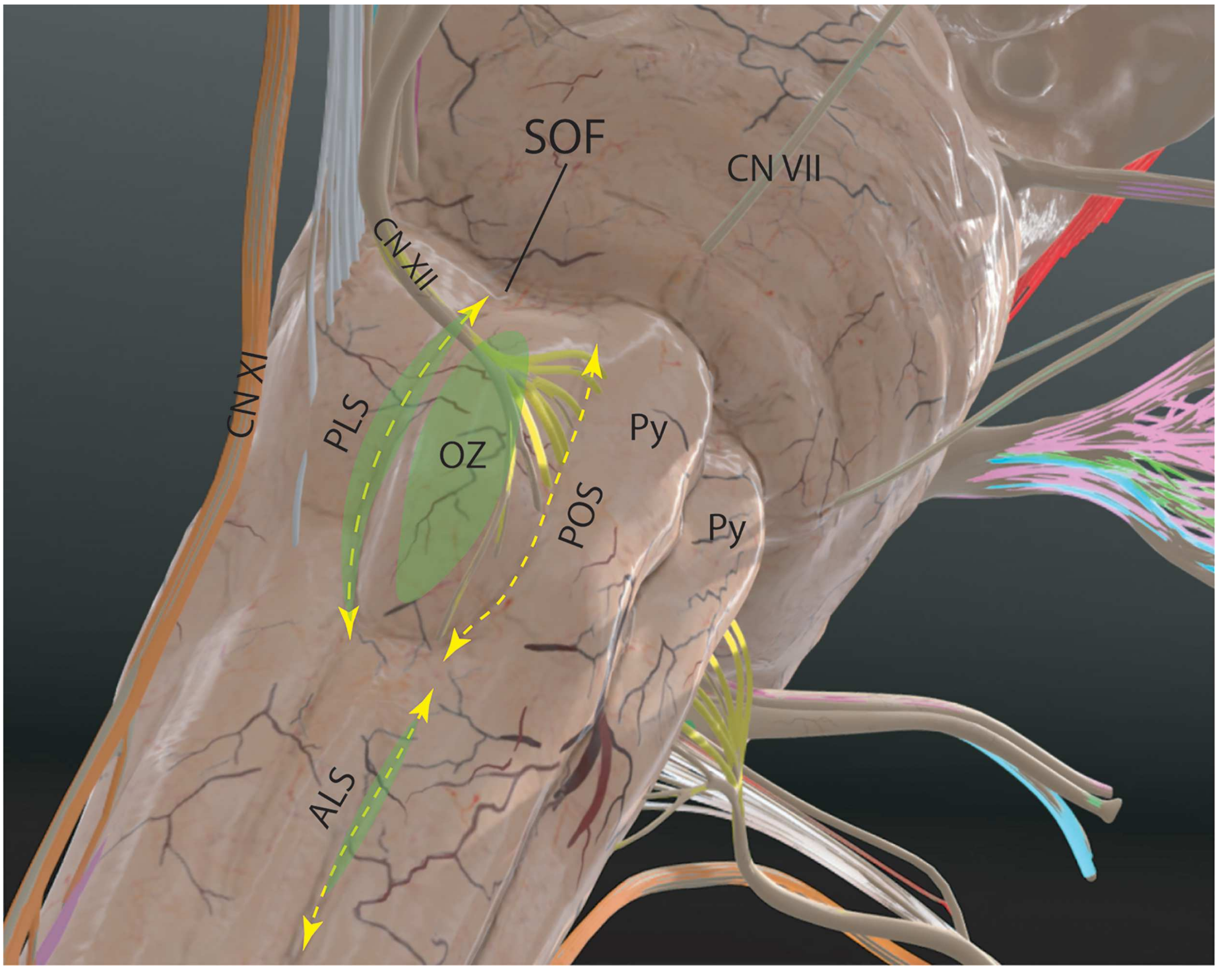

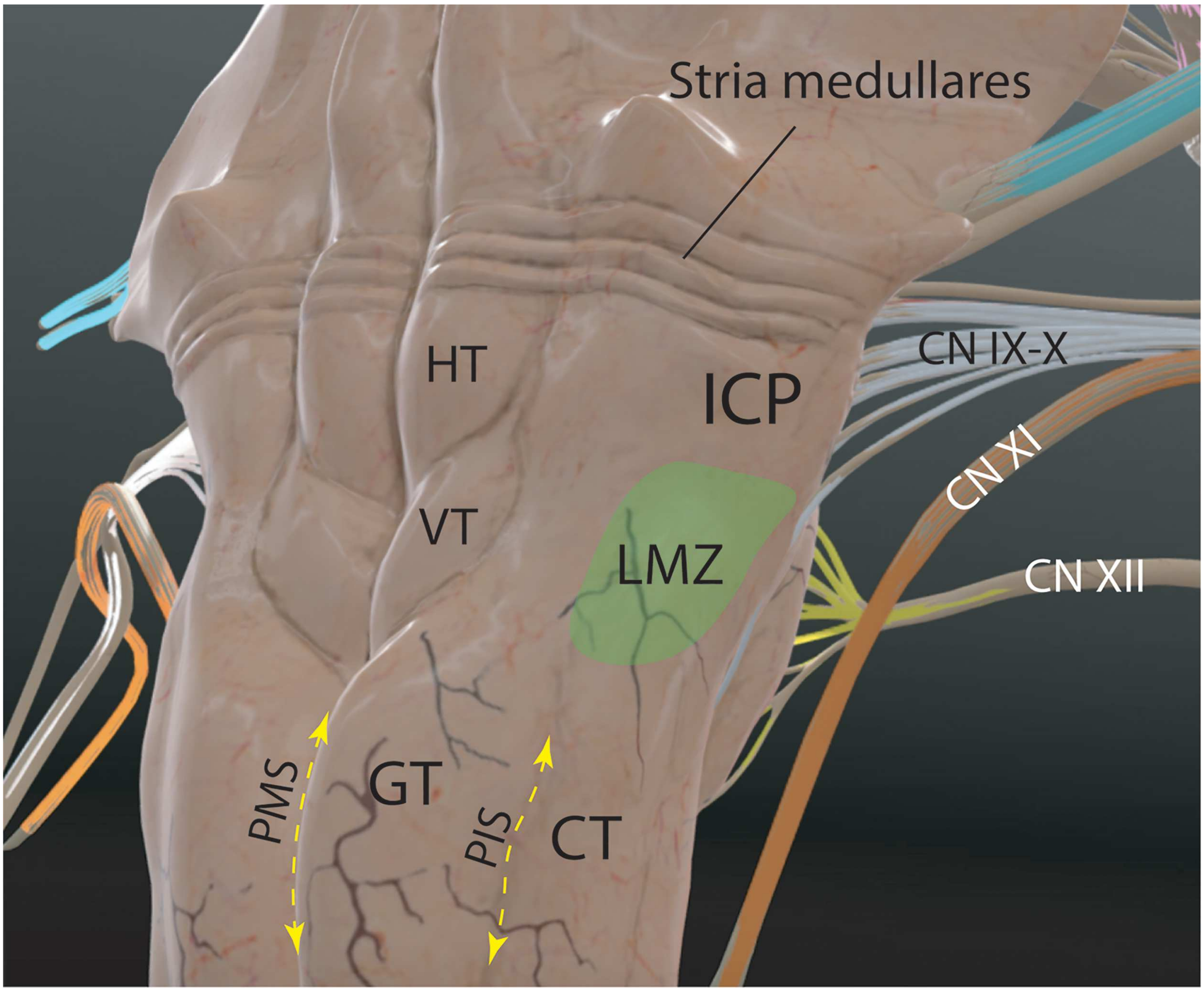
Stria medullares
HT
ICP
CN IX-X
CN XI
VT
LMZ
CN XII
PMS
GT
PIS
CT

Model 1: Three-dimensional (3D) model showing the reconstructed anatomy of the external and internal structure of the midbrain with relevant safe entry zones. (The instructions for use of this model are as follows: Please use the full-screen function for optimal visualization [by clicking on the arrows on the right lower corner of the model]. To move the model in 3D space, use your mouse's left click and drag; to enlarge or decrease the size of the object, use the mouse's wheel. The right click and drag function moves the model across the plane.) Please click on "Select an annotation" link at the bottom of the window and "Show annotations" so that the anatomical labels become visible. With permission from *The Neurosurgical Atlas* by Aaron Cohen-Gadol, MD. (https://sketchfab.com/3d-models/midbrain-labeled-cda12a620a7c4b65b7067d55d4e79294)

Model 2: Three-dimensional model showing the reconstructed anatomy of the external and internal structure of the pons with relevant safe entry zones. Please click on “Select an annotation” link at the bottom of the window and “Show annotations” so that the anatomical labels become visible. With permission from *The Neurosurgical Atlas* by Aaron Cohen-Gadol, MD. (https://sketchfab.com/3d-models/pons-labeled-d876bd93e3134c18a1edb981e270e2e2)

Model 3: Three-dimensional model showing the reconstructed anatomy of the external and internal structures of the medulla oblongata with relevant safe entry zones. Please click on “Select an annotation” link at the bottom of the window and “Show annotations” so that the anatomical labels become visible. With permission from *The Neurosurgical Atlas* by Aaron Cohen-Gadol, MD. (https://sketchfab.com/3d-models/medulla-labeled-4f405fd9dc2b4074aeec2c04ae50a814)

Table 1. Summary of safe entry zones to the brainstem and surgical approaches used to access them

SEZ	Definition/Boundaries	Cisternal Relationship	Surgical Approach(es)
Midbrain			
AMZ	Medial one-fifth of the ventral aspect of the crus cerebri lateral to the root exit zone of the oculomotor nerve, between the superior cerebellar and posterior cerebral arteries	Crural	PTTS, ST, ETC and PT
LMS	Between the cerebral peduncle anteriorly and the midbrain tegmentum posteriorly	Ambient (posterior)	ST, SCIT (paramedian, extreme-lateral), RS, PS
Supra-CZ	Above the superior colliculi at the subpineal triangle (of Obersteiner)	Quadrigeminal	SCIT
Infra-CZ	Below the inferior colliculi	Quadrigeminal	SCIT
Inter-CZ	Vertical cleft between the left and right colliculi	Quadrigeminal	SCIT
Pons			
PTZ	Ventral aspect of pons, medial to the trigeminal-facial line and lateral to the pyramidal fibers	Prepontine	RS, PS, ST and AP, ETC and EDAP
STZ	Superior to the CN V REZ lateral to the pyramidal tract	Cerebellopontine, prepontine	RS, PS, ST and AP, ETC and EDAP, ST, PTTS
LPZ	Ventrolateral aspect of pons, lateral to the trigeminal-facial line	Cerebellopontine	RS, PS
SFZ	Suprafacial triangle delimited by the superior cerebellar peduncle laterally, the MLF medially, and the facial colliculus inferiorly	Fourth ventricle	TV, TeV
IFZ	Between the facial colliculus superiorly and the hypoglossal and vagal triangles inferiorly	Fourth ventricle	TV, TeV
MS-IV	Between the bilateral median eminences above the level of facial colliculi	Fourth ventricle	TV, TeV
AA	Inferior cerebellar peduncle fibers located underneath the lateral end of the striae medullares at the region of the lateral recess of the fourth ventricle	Lateral recess of the fourth ventricle	TBF, TeV, TUT
FP	Rostral wall of the lateral recess of the fourth ventricle just rostral to the	Lateral recess of the fourth ventricle	TBF, TeV, TUT

	attachment of the inferior medullary velum to the flocculus		
Medulla			
ALS	Preolivary sulcus between the caudal-most roots of the hypoglossal nerve and the rostral-most rootlets of the C1 nerve	Cerebellomedullary	FL, ETC and pC
PLS	Postolivary sulcus, anterior to the rootlets of CN IX–X	Cerebellomedullary	FL
LMZ	Rostrolateral part of the inferior cerebellar peduncle dorsal to the foramen of Luschka and REZs of CN IX–X	Cerebellomedullary (rostral part), cerebellopontine	RS, PS, FL
PMS	Between the gracile fascicles	Magna	MSO and C1 laminectomy
PLS	Between the gracile and cuneate tubercles/fascicles	Magna	MSO and C1 laminectomy

AA, area acustica; ALS, anterolateral sulcus; AMZ, anterior mesencephalic zone; AP, anterior petrosectomy; CN, cranial nerve; CZ, collicular zone; EDAP, extradural anterior petrosectomy; ETC, endoscopic transclival; FL, far lateral; FP, floccular peduncle; IFZ, Infrafacial zone; LMS, lateral mesencephalic zone; LMZ, lateral medullary zone; LPZ, lateral pontine zone; MLF, medial longitudinal fasciculus; MS-IV, median sulcus of fourth ventricle; MSO, midline suboccipital approach; pC, partial condylectomy; PLS, posterolateral sulcus; PMS, posterior median sulcus; PS, presigmoid; PT, pituitary transposition; PTTS, pretemporal trans-Sylvian; PTZ, peritrigeminal zone; REZ, root entry/exit zone; RS, retrosigmoid; SCIT, supracerebellar infratentorial; SFZ, suprafacial zone; ST, subtemporal; STZ, supratrigeminal zone; TBF, tonsillobiventral fissure; TeV, telovelar; TUT, trans-uvulotonsillar; TV, transvermian.